Contents lists available at ScienceDirect

Engineering Analysis with Boundary Elements

journal homepage: www.elsevier.com/locate/enganabound

On the increasingly flat radial basis function and optimal shape parameter for the solution of elliptic PDEs

C.-S. Huang [a,*], H.-D. Yen [a], A.H.-D. Cheng [b]

[a] Department of Applied Mathematics, National Sun Yat-Sen University, Kaohsiung 804, Taiwan, ROC
[b] School of Engineering, University of Mississippi, University, MS 38677, USA

ARTICLE INFO

Article history:
Received 5 January 2010
Accepted 10 March 2010

Keywords:
Multiquadric collocation method
Meshless method
Error estimate
Arbitrary precision computation
Increasingly flat radial basis function

ABSTRACT

For the interpolation of continuous functions and the solution of partial differential equation (PDE) by radial basis function (RBF) collocation, it has been observed that solution becomes increasingly more accurate as the shape of the RBF is flattened by the adjustment of a shape parameter. In the case of interpolation of continuous functions, it has been proven that in the limit of increasingly flat RBF, the interpolant reduces to Lagrangian polynomials. Does this limiting behavior implies that RBFs can perform no better than Lagrangian polynomials in the interpolation of a function, as well as in the solution of PDE? In this paper, arbitrary precision computation is used to test these and other conjectures. It is found that RBF in fact performs better than polynomials, as the optimal shape parameter exists not in the limit, but at a finite value.

1. Introduction

To explore the efficiency of scattered data interpolation, Franke [1] compared 29 interpolation algorithms on a set of continuous functions. He concluded that Hardy's [2,3] multiquadric radial basis function collocation "*yields consistently good result, often giving the most accurate results of all tested methods*." This finding has stimulated a growing interest in using radial basis functions (RBFs) for interpolating continuous functions. Based on the similar idea, Kansa [4,5] was the first to apply RBF collocation for solving partial differential equations (PDEs). RBF collocation method has since become a popular tool for solving a wide range of engineering problems, including shallow water equation [6], biphasic mixtures [7], convective–diffusive solid–liquid phase change [8], plate theory [9], and ill-posed boundary value problems [10].

As observed by Kansa [4,5] for solving PDE, and Tartwater [11] for interpolating functions, the accuracy of the approximated solution/function significantly improves when the multiquadric function is made increasingly flat, by increasing the value of its shape parameter c. Madych [12] provided an error estimates that states $\varepsilon \sim \mathcal{O}(e^{ac}\lambda^{c/h})$, where h is the distance between collocation nodes (mesh size), a is a positive constant, and $0<\lambda<1$, for the interpolation of band limited functions. The above expression suggests exponential convergence for error, and as $c \to \infty$, the error $\varepsilon \to 0$. This conjecture was tested for the solution of partial differential equation, first by Cheng et al. [13], and later by Huang et al. [14] using arbitrary precision computation.

On another line of research, Baxter [15], Driscoll and Fornberg [16], Fornberg et al. [17], Larsson and Fornberg [18], and Schaback [19], studied the limiting behavior of the multiquadric and Gaussian interpolants. They proved mostly for univariate functions, and conjectured for multivariate functions, that in the limit of $\epsilon \to 0$ ($\epsilon = 1/c$), the interpolants reduce to polynomials with finite number of terms. With such observation, it seems natural to ask: does this type of limiting behaviors implies that RBFs can perform no better than polynomials in the interpolation of function, and in the solution of PDE?

Analogous to RBF collocation for solution of PDE, the method of fundamental solutions (MFS) [20] uses fundamental solutions, instead of RBF, as the basis function. It was observed that as the radius of the circle for distributing the fundamental solutions, R, becomes larger and larger, thus making the portion of the fundamental solution used for interpolation increasingly flat, the solution accuracy increases. It was also proven that as $R \to \infty$, the interpolant degenerates into a harmonic polynomial [21–23], which are the basis functions used in Trefftz method [24,25]. Due to this limiting behavior, it has been suggested that MFS can be no better than the Trefftz method.

In this paper, we shall examine the RBF collocation method and the theoretically predicted degeneracy behavior of multiquadric and Gaussian basis functions associated with their flatness. As mentioned above, the theories are proven mostly for interpolation of univariate functions. Their behavior in multiple dimensions, and for the solution of partial differential equations, remains a speculation or conjecture. Hence in this paper we are

[*] Corresponding author.
E-mail address: huangcs@math.nsysu.edu.tw (C.-S. Huang).

0955-7997/$ - see front matter © 2010 Elsevier Ltd. All rights reserved.
doi:10.1016/j.enganabound.2010.03.002

interested in testing the following conjectures by numerical evidences:

- In the multivariate interpolation and the solution of PDE, as the basis function becomes infinitely flat ($c \to \infty$), does the error diverge, approach to zero, or approach to a finite limit by degenerating into a finite term polynomial?
- When a finite limit for the error exists as $c \to \infty$, is this limit the optimal error bound, or does there exist a minimum error at a finite, optimal value of c?

It is well known that, as the basis function becomes increasingly flat, the error generally reduces exponentially. At the same time, however, it is observed that the matrix condition number increases exponentially. Using a traditional, finite precision computer program, the computation will break down when the condition number becomes too large. For this reason, these theories and conjectures stated above remain largely untested. In this paper, such difficulty is overcome by using the arbitrary precision computation technique pioneered in Huang et al. [14].

A conclusion of this study is that, as $c \to \infty$, the RBF interpolant can either converge to a polynomial limit, or it can diverge. Whether a finite error bound exists or not is dependent on the basis function used, the interpolation node pattern, and the function interpolated. Another conclusion is that the minimum error for the interpolant is not located at $c \to \infty$. Rather, there exists a finite, optimal value of c, where the error is minimum.

2. Radial basis function collocation method

2.1. Radial basis functions

A radial function is a multivariate function Φ such that

$$\Phi : \mathbb{R}^d \to \mathbb{R} \quad \text{in the sense that } \Phi(x_1,\ldots,x_d) \to \phi(\|(x_1,\ldots,x_d)\|_2). \tag{1}$$

Here the 2-norm of $\mathbf{x} = (x_1,\ldots,x_d)$ is

$$\|\mathbf{x}\|_2 = \sqrt{\sum_{i=1}^{d} x_i^2} = r, \tag{2}$$

i.e., the Euclidean distance of $\mathbf{x}$ to the origin (radial distance).

RBF collocation method is an "element-free", or a "meshless", technique for generating data-dependent spaces of multivariate functions. The spaces are spanned by shifted and scaled radial functions. The shifting is accomplished by using a set of scattered *centers*, $\mathbf{y}_1,\ldots,\mathbf{y}_n$ in $\mathbb{R}^d$, sometimes called *basis points*, as the origin of the RBFs. Reconstruction of functions is then made by trial functions which are linear combinations

$$u(\mathbf{x}) := \sum_{j=1}^{N} \lambda_j \Phi(\mathbf{x},\mathbf{y}_j) = \sum_{j=1}^{N} \lambda_j \phi(\|\mathbf{x}-\mathbf{y}_j\|_2). \tag{3}$$

Some of the commonly used RBFs are given in Table 1. All of these RBFs can be scaled by a shape parameter c, or $\in = 1/c$, that controls the flatness (or steepness) of the RBF. This is done in such a way that $\phi(r)$ is replaced by $\phi(\in r)$, or $\phi(r/c)$. For example, the MQ is scaled as $\phi = \sqrt{(\in r)^2+1}$, or $\phi = \sqrt{(r/c)^2+1}$. The effect of the scaling is that as $\in$ gets smaller, or c gets larger, the RBF becomes flatter. In the present paper, we only utilize Gaussian (GA) and inverse multiquadric (IMQ) as our basis functions. These basis functions are positive definite, such that no augmentation by polynomial terms is needed. Further detail on RBF can be found in two excellent books, by Buhmann [26] and Wendland [27].

Table 1
Some examples of radial basis functions.

Infinitely smooth RBFs	
RBF	$\phi(r)$
Gaussian (GA)	e^{-r^2}
Multiquadric (MQ)	$\sqrt{r^2+1}$
Inverse multiquadric (IMQ)	$1/\sqrt{r^2+1}$
Inverse quadric (IQ)	$1/(r^2+1)$

2.2. Interpolation

A typical interpolation problem has the following form: Given scattered data points $\mathbf{y}_j$, $j=1,\ldots,N$, and data values $u_j = u(\mathbf{y}_j)$, find an interpolant

$$s(\mathbf{x}) = \sum_{j=1}^{N} \lambda_j \phi(\|\mathbf{x}-\mathbf{y}_j\|_2). \tag{4}$$

The interpolation at collocation points gives

$$s(\mathbf{y}_i) \equiv \sum_{j=1}^{N} \lambda_j \phi(\|\mathbf{y}_i-\mathbf{y}_j\|_2) = u_i, \quad i = 1,\ldots,N. \tag{5}$$

The above can be summarized into a system of equations for the unknown coefficients λ_j,

$$\mathbf{A}\Lambda = \mathbf{u}, \tag{6}$$

where $\mathbf{A}$ is an $N \times N$ matrix with elements $A_{ij} = \phi(\|\mathbf{y}_i-\mathbf{y}_j\|_2)$, $\Lambda = (\lambda_1,\ldots,\lambda_N)^T$, and $\mathbf{u} = (u_1,\ldots,u_N)^T$. The solvability of such system, with distinct centers, was proven by Micchelli [28].

2.3. Partial differential equation

For simplicity, we shall discuss only the solution of Dirichlet boundary value problem of Poisson's equation here. Let $\Omega \subset \mathbb{R}^d$ be a d-dimensional domain and let $\partial\Omega$ be the boundary of the domain. Given the following Poisson's equation:

$$\Delta u(\mathbf{x}) = f(\mathbf{x}), \quad \mathbf{x} \in \Omega, \tag{7a}$$

$$u(\mathbf{x}) = g(\mathbf{x}), \quad \mathbf{x} \in \partial\Omega, \tag{7b}$$

we seek its approximate solution in the form of (4). Now take a set of N_1 distinct points $\mathbf{y}_i \in \Omega$, and a set of $N-N_1$ distinct points $\mathbf{y}_i \in \partial\Omega$, as centers, as well as collocation points, and we enforce

$$\Delta s(\mathbf{y}_i) \equiv \sum_{j=1}^{N} \lambda_j \Delta\phi(\|\mathbf{y}_i-\mathbf{y}_j\|_2) = f(\mathbf{y}_i), \quad i = 1,\ldots,N_1, \tag{8a}$$

$$s(\mathbf{y}_i) \equiv \sum_{j=1}^{N} \lambda_j \phi(\|\mathbf{y}_i-\mathbf{y}_j\|_2) = g(\mathbf{y}_i), \quad i = N_1+1,\ldots,N. \tag{8b}$$

This corresponds to a system of equations with an unsymmetric coefficient matrix, schematically structured as

$$\left[\frac{\Delta\phi}{\phi}\right][\Lambda] = \left[\frac{f}{g}\right]. \tag{9}$$

Similar to the interpolation problem, we shall have an unique solution for this system.

Since the condition number of the matrix system in (6) and (9) grows rapidly as the shape factor $\in \to 0$, we use the arbitrary precision computation capability of *Mathematica* to evaluate the matrices.

2.4. Error measures

To assess the solution error, we devise an L^2-norm as the normalized root mean square (RMS) error

$$\varepsilon_{\mathrm{RMS}}(s,u)=\frac{\sqrt{(1/n)\sum_{i=1}^{n}[u(\mathbf{x}_i)-s(\mathbf{x}_i)]^2}}{|u_{\max}|}, \tag{10}$$

where u is the exact solution (either for interpolation or PDE), s is the approximate solution, $\mathbf{x}_i$, $i=1,\ldots,n$ are observation points uniformly distributed over the domain, and n is a large number, typically taken as 100 N, with N the number of collocation nodes. Note that $\varepsilon_{\mathrm{RMS}}$ is normalized by the maximum value of the exact solution to give a sense of percentage error.

3. One-dimensional interpolation and PDE

For a one-dimensional approximation, (4) becomes

$$s(x,\in)=\sum_{j=1}^{N}\lambda_j\phi(|x-y_j|,\in), \tag{11}$$

where we have explicitly brought out the role of $\in$ $(=1/c)$ in the approximation. Driscoll and Fornberg [16] pointed out that the RBFs presented in Table 1 belong to a class of infinitely smooth RBFs that can be expanded into a power series

$$\phi(x,\in)=a_0+a_1(\in x)^2+a_2(\in x)^4+\cdots=\sum_{i=o}^{\infty}a_i(\in x)^{2i} \tag{12}$$

with the coefficients given in Table 2. They have also proven that, for this class, if the interpolation system defined by (5) and (6) is nonsingular, then the interpolant (11) satisfies

$$\lim_{\in\to 0}s(x,\in)=L_N(x)+\mathcal{O}(\in^2), \tag{13}$$

where $L_N(x)$ is a Lagrangian interpolating polynomial of N th degree with $L_N(y_i)=u(y_i)$ on the nodes. The special cases of $N\le 3$ were explicitly demonstrated in [16].

We shall demonstrate below that similar result as (13) exists for the solution of one-dimensional differential equations. First, for the special cases of $N\le 2$, the convergence of the approximate solution of differential equation to Lagrangian polynomial with $\varepsilon\sim\mathcal{O}(\in^2)$ has been proven by Yen [29]. In the following, we shall test the conjecture (13) for solving one-dimensional differential equation through numerical examples, for the cases of $N>3$.

Given the Dirichlet boundary value problem of (1-D) Poisson's equation,

$$\frac{d^2u}{dx^2}=f(x),\quad x_L\le x\le x_R,$$

$$u(x_L)=u_L,\quad u(x_R)=u_R, \tag{14}$$

we seek the approximate solution in the form of (11).

Table 2
Expansion coefficients for infinitely smooth RBFs.

RBF	Coefficients	
GA	$a_i=\frac{(-1)^i}{i!}$,	$i=0,\ldots$
MQ	$a_0=1,\ a_i=\frac{(-1)^{i+1}}{2i}\prod_{k=1}^{i-1}\frac{2k-1}{2k}$,	$i=1,\ldots$
IMQ	$a_0=1,\ a_i=(-1)^i\prod_{k=1}^{i}\frac{2k-1}{2k}$,	$i=1,\ldots$
IQ	$a_i=(-1)^i$,	$i=0,\ldots$

3.1. Example 3.1

For $0\le x\le 1$, two functions, $u=\cos 2\pi x$ and $u=e^{10x}$, as the exact solution of (14), are tested, using IMQ and GA. The right hand side of Poisson's equation and the boundary conditions in (14) are defined from the exact solution; that is, $f(x)=-4\pi^2\cos 2\pi x$ and $f(x)=100\ e^{10x}$, respectively. The problems are solved using different number of interpolation terms, N, for a range of $\in$ values; and the results are presented in Tables 3 and 4. In order to observe the convergence of the RBF interpolants to polynomials, in Tables 3 and 4 we presented not the RBF error with respect to the exact solution u, but with a polynomial interpolation using the same number of terms, $\tilde{s}$, expressed in terms of the RMS error, $\varepsilon_{\mathrm{RMS}}(s,\tilde{s})$, as defined in (10).

In Table 3, we observe that the RBF interpolant does approach the polynomial limit as $\in\to 0$. In fact, the difference between them decreases as $\varepsilon(s,\tilde{s})\sim\mathcal{O}(\in^2)$, the same as that predicted by (13). This is an indication that the error estimates for the interpolation and for the PDE are similar. In the table, we also observe that as N becomes larger, the difference between the RBF and polynomial interpolants seems to decrease. Another observation from Table 3 is that the GA approaches the polynomial limit faster than the IMQ.

In Table 4, the same error analysis is presented for the solution $u(x)=e^{10x}$. The same observations as in Table 3 are made here.

Table 3
Difference between RBF and polynomial interpolants, $\varepsilon(s,\tilde{s})$, for $u(x)=\cos 2\pi x$, as function of $\in$ and N.

$\in$	N			
	3	5	8	18
IMQ				
10^{-1}	9.57(−03)	2.70(−03)	2.12(−04)	9.11(−12)
10^{-2}	9.71(−05)	2.77(−05)	2.24(−06)	1.58(−13)
10^{-3}	9.71(−07)	2.77(−07)	2.24(−08)	1.59(−15)
10^{-4}	9.71(−09)	2.77(−09)	2.24(−10)	1.59(−17)
GA				
10^{-1}	2.48(−03)	4.97(−04)	3.08(−05)	9.96(−13)
10^{-2}	2.48(−05)	4.99(−06)	3.10(−07)	1.03(−14)
10^{-3}	2.48(−07)	4.99(−08)	3.10(−09)	1.03(−16)
10^{-4}	2.48(−09)	4.99(−10)	3.10(−11)	1.03(−18)

Table 4
Difference between RBF and polynomial interpolants, $\varepsilon(s,\tilde{s})$, for $u(x)=e^{10x}$, as function of $\in$ and N.

$\in$	N			
	3	5	8	18
IMQ				
10^{-1}	1.08(−03)	6.79(−04)	1.25(−04)	7.78(−10)
10^{-2}	1.09(−05)	6.83(−06)	1.24(−06)	6.37(−12)
10^{-3}	1.09(−07)	6.83(−08)	1.24(−08)	6.35(−14)
10^{-4}	1.09(−09)	6.83(−10)	1.24(−10)	6.35(−16)
GA				
10^{-1}	2.91(−04)	1.28(−04)	1.71(−05)	4.17(−11)
10^{-2}	2.91(−06)	1.28(−06)	1.71(−07)	4.11(−13)
10^{-3}	2.91(−08)	1.28(−08)	1.71(−09)	4.11(−15)
10^{-4}	2.91(−10)	1.28(−10)	1.71(−11)	4.11(−17)

4. Interpolation by IMQ with uniform grid

In this section we test the interpolation of smooth functions in two dimensions using inverse multiquadric (IMQ). The functions are defined in a unit square $[0,1]\times[0,1]$. The RBF centers, which are also the collocation points, are laid on an uniformly spaced Cartesian grid. The grid spacing, that is, the Cartesian distance between two points, is defined as h. A number of different functions are tested. A few representative results are reported in the following.

4.1. *Example 4.1*

In this first example, we use IMQ to interpolate the function $u=\sin(2\pi x)+\cos(2\pi y)$. A 21×21 uniform grid is laid over the unit square domain, to give a mesh size $h=1/20$. The interpolation is performed using a whole range of c values, and the RMS error as defined in (10) is calculated. The result is reported in Figs. 1 and 2 using different plotting ranges and scales.

In Fig. 1, we have carried out the computation for the shape parameter c to as large as 10^6. We observe that the error reaches an asymptotic value of about 10^{-14}. This behavior suggests that the IMQ interpolant has a limit, and possibly a bivariate polynomial limit, as $\epsilon\to 0$. This observation is not surprising, as the function interpolated, $u=\sin(2\pi x)+\cos(2\pi y)$, is essentially the linear combination of two one-dimensional functions, in the two Cartesian axes, and the grid used for interpolation is aligned along these two axes.

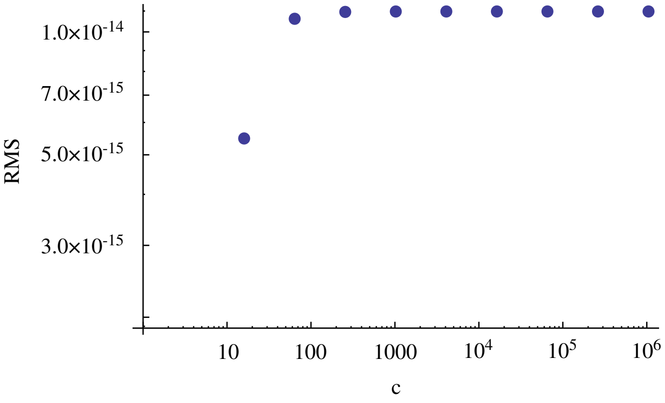

Fig. 1. RMS error $\varepsilon_{\mathrm{RMS}}(s,u)$ for interpolating $u=\sin(2\pi x)+\cos(2\pi y)$ using IMQ: mesh size $h=1/20$, in large c range.

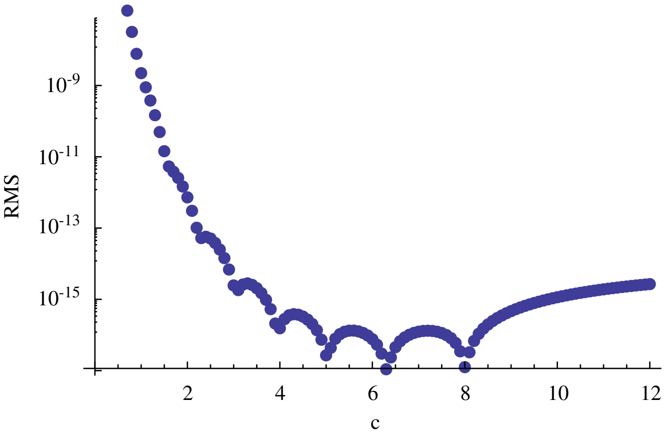

Fig. 2. RMS error $\varepsilon_{\mathrm{RMS}}(s,u)$ for interpolating $u=\sin(2\pi x)+\cos(2\pi y)$ using IMQ: mesh size $h=1/20$, in smaller c range.

With the existence of such limit, a misconception may develop that the RBF interpolations can perform no better than polynomial interpolation. In Fig. 1, however, we observe that the error limit is approached from below, meaning that the error *increases* to that limit. This indicates that the best performance of the interpolant is not at $c\to\infty$, but at some finite value. In Fig. 2, we plot the same result in the smaller c range. In this plot, we observe that as c increases, the error decreases first, before it increases. A minimum error of about 10^{-16}–10^{-17}, which is two to three orders of magnitude smaller than the polynomial error limit, occurred between $4<c<8$. This observation suggests that if an optimal c value can be located, then IMQ is much more efficient than polynomial as a basis function for interpolation.

4.2. *Example 4.2*

As a confirmation of polynomial limit, we have tested a number of polynomial functions, with only one example given here as an illustration. For the case $u=x^2y$, we use a uniform grid with $h=1/10$ for interpolation. The resultant error is shown in Fig. 3. We observe that as c continues to increase, the error decreases without reaching a finite limit. In this plot, the RMS error approaches zero at the rate $\varepsilon\sim\mathcal{O}(\epsilon^8)$ as $\epsilon\to 0$. The same behavior is observed for a number of bivariate polynomials tested.

4.3. *Example 4.3*

We now use IMQ to interpolate $u=\sin(2\pi x)\cos(2\pi y)$ over the unit square. As compared to the case $u=\sin(2\pi x)+\cos(2\pi y)$ in Example 4.1, the current function is a true bivariate function, not a linear combination of univariate functions.

Results of the interpolation are presented in Figs. 4 and 5. In Fig. 4, over the smaller c range, we observe a behavior similar to Fig. 2 in Example 4.1, with optimal c located between 4 and 8, with a minimum error about 10^{-16}.

For large c, however, Fig. 5 shows a very different result: the error grows without bound as $c\to\infty$. That is, the IMQ interpolant diverges as $\epsilon\to 0$. Similar divergent behavior is observed for several other transcendental functions tested, such as different combinations of trigonometric and exponential functions, over various uniform grid sizes.

Driscoll and Fornberg [16] in fact reported this result: using MQ interpolation on a $[0,1]\times[0,1]$ square using a uniform grid with $h=1/5$, they found that the error diverges at the rate of

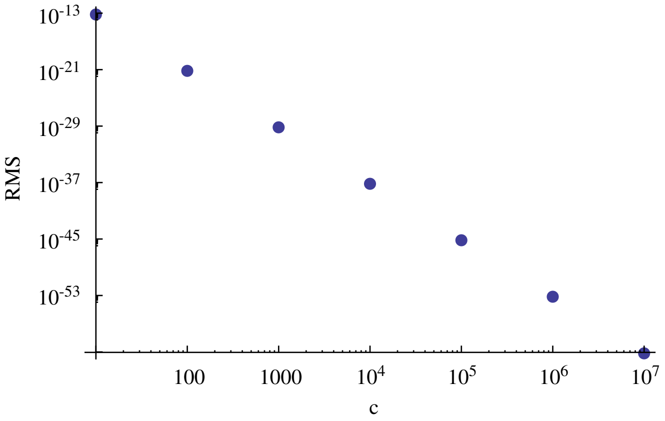

Fig. 3. RMS error $\varepsilon_{\mathrm{RMS}}(s,u)$ for interpolating $u=x^2y$ using IMQ: mesh size $h=1/10$, in large c range.

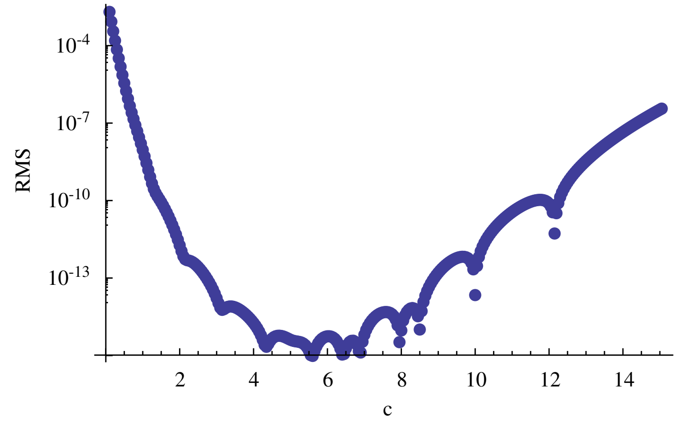

Fig. 4. RMS error $\varepsilon_{\text{RMS}}(s,u)$ for interpolating $u=\sin(2\pi x)\cos(2\pi y)$ using IMQ: mesh size $h=1/20$, in smaller c range.

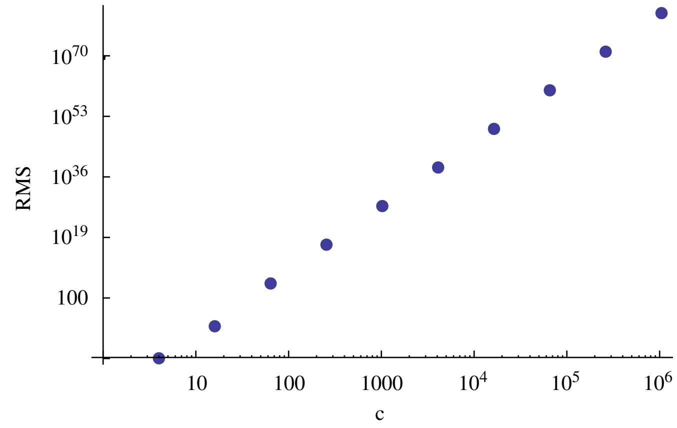

Fig. 5. RMS error $\varepsilon_{\text{RMS}}(s,u)$ for interpolating $u=\sin(2\pi x)\cos(2\pi y)$ using IMQ: mesh size $h=1/20$, in large c range.

$\varepsilon \sim \mathcal{O}(\in^{-2})$ as $\in \to 0$, *for arbitrary functions*. In the current case, with $h=1/20$, the divergence rate appears to be $\varepsilon \sim \mathcal{O}(\in^{-17})$. Larsson and Fornberg [18] also reported that for IMQ, MQ and IQ, the divergence behavior can be found on nonuniform, but specially patterned, grids, such as along a single diagonal line.

We shall observe in Section 5 that, if this same function is interpolated using GA instead of IMQ, the interpolant actually converges as $\in \to 0$. Also, in Section 7, we demonstrate that convergence can be achieved using a random distribution of collocation nodes with the IMQ interpolation.

It is of interest to observe that in the three examples, Examples 4.1–4.3, we used the same basis function (IMQ), and the same uniform interpolation grid. This means that the interpolation matrix **A** in (6) is identical for all three cases. In the limit of $\in \to 0$, the condition number for **A**, as well as the coefficient vector $\Lambda=(\lambda_1,\ldots,\lambda_N)^T$, diverges. However, as we already demonstrated in Examples 4.1 and 4.2, the interpolant can converge to a finite limit. According to Driscoll and Fornberg [16] and Larsson and Fornberg [18], whether the interpolant has a finite limit of not is dependent only on the choice of the basis function and the grid arrangement. However, as observed in the cases here, the divergent behavior of the interpolant is also dependent on the function to be interpolated, that is, the right hand side vector **u**. We observe that if the function to be interpolated is of one-dimensional nature, aligned with the grid axes, or if the function is a bivariate polynomial, the interpolant converges. Otherwise, it diverges for IMQ interpolation.

It is of interest to point out that, for practical applications, the divergent behavior of IMQ interpolant on a uniform grid as $c\to\infty$ is generally not a cause of concern. As we observe in Fig. 4 that at smaller c values an optimal c exists, where the error is minimum. Our goal is to seek such value and not to carry the computation much beyond that value to $c\to\infty$. Also, we shall demonstrated in Section 7 that this divergent behavior seems to disappear if a random distribution of collocation nodes is used.

5. Interpolation by GA with uniform grid

In the above section, we have been using the IMQ as the basis function. In this section, we shall replace IMQ by the Gaussian (GA) basis function.

5.1. Example 5.1

The same three functions tested in Examples 4.1–4.3 are tested here. For the two cases, $u=\sin(2\pi x)+\cos(2\pi y)$ and $u=x^2y$, we observe the similar error pattern as reported in Figs. 1–3, but with better accuracy. These results are not shown here.

For the function $u=\sin(2\pi x)\cos(2\pi y)$, as investigated in Example 4.3, we observe, in the smaller c range, a similar behavior as Fig. 4; that is, an optimal c exists where the error is minimum. In the large c range, however, the error approaches a finite limit as $c\to\infty$, as shown in Fig. 6. This behavior is different from the divergent error shown in Fig. 5, for IMQ interpolant. In fact, after testing several other transcendental functions interpolated by GA, no divergent behavior was found as $c\to\infty$.

The above observation is consistent with Theorem 3.2 presented in Fornberg et al. [17], which states: *In the case when the data points are laid out in a finite rectangular lattice (in any number of dimensions), GA interpolants will not diverge as* $\in \to 0$.

6. Solution of PDE with uniform grid

As demonstrated in Sections 2.2 and 2.3, the approximation processes for interpolation of a function and the solution of a PDE are similar—the same interpolant is used to approximate the function and the solution of PDE. The difference is, for interpolation, we collocate at a set of points the values of the function; while for the solution of PDE, the collocation is conducted for a mixture of the function values at boundary locations (for Dirichlet boundary condition), and second derivatives of the function (governing equation) over the solution domain. Hence, it is of interest to observe whether the error behavior remains the same. In Section 3, we have demonstrated that, for univariate functions,

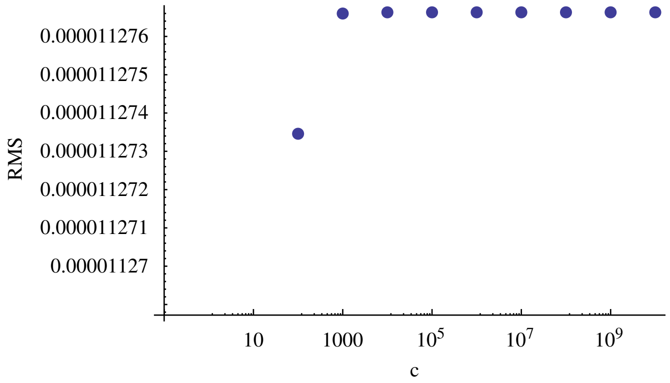

Fig. 6. RMS error $\varepsilon_{\text{RMS}}(s,u)$ for interpolating $u=\sin(2\pi x)\cos(2\pi y)$ using GA: mesh size $h=1/10$, in large c range.

Please cite this article as: Huang C-S, et al. On the increasingly flat radial basis function and optimal shape parameter for the solution of elliptic PDEs. Eng Anal Bound Elem (2010), doi:10.1016/j.enganabound.2010.03.002

the error behaviors for interpolation and the solution of one-dimensional differential equation are the same. In the following set of examples, we shall solve two-dimensional boundary value problems of Poisson's equation to test these conjectures.

6.1. Example 6.1

In this example, we try to find the approximate solution of a boundary value problem of Poisson's equation, defined as (7), over the unit square [0,1] × [0,1]. The exact solution of this problem is $u(x,y)=\sin(2\pi x)+\cos(2\pi y)$, which is the same function as that interpolated in Example 4.1. The boundary value problem is created by substituting the exact solution into (7) to find $f(\mathbf{x})$ and $g(\mathbf{x})$. For example, $f(\mathbf{x})$ in this case is $f(x,y)=-4\pi^2[\sin(2\pi x)+\cos(2\pi y)]$. IMQ is used as the basis function and the collocation points are laid over the same uniform Cartesian grid as Example 4.1, with $h=1/20$. The error as a function of the shape parameter c is plotted as Figs. 7 and 8.

First, we observe that the RMS error has the same pattern as Figs. 1 and 2; that is, it has a minimum error at a finite c, and it approaches an asymptotic limit as $c\to\infty$. However, the asymptotic limit of the PDE case is about two orders of magnitude larger than the interpolation case. The minimum error is located in the same range of c value, but its magnitude is about one order of magnitude greater in the PDE case.

6.2. Example 6.2

Next we test the boundary value problem of Poisson's equation whose exact solution is $u(x,y)=\sin(2\pi x)\cos(2\pi y)$ over the unit square [0,1] × [0,1], corresponding to Example 4.3. The same basis function (IMQ) and uniform grid size ($h=1/20$) are used.

First, we observe in Fig. 9 that the error behavior is similar to Fig. 4—they both show an optimal c located in the same range, with a minimum error of about 10^{-16}. In Fig. 10, we find that the error diverges to infinity, similar to Fig. 5 for the interpolation problem. The rate of error divergence is $\varepsilon\sim\mathcal{O}(\in^{-13})$, as compared to $\mathcal{O}(\in^{-17})$ for the interpolation case.

In this and the preceding examples, we again show that the existence of a finite limit for the interpolant as $c\to\infty$ is dependent on the function to be interpolated. We also observe that such error behavior, whether it is divergent or convergent, seems to be not affected by its collocation algorithm, either directly collocated for function values, or for a combination of function values and its derivatives.

6.3. Example 6.3

We now use GA to solve Poisson's equation over the unit square domain with the same exact solution $u=\sin(2\pi x)\cos(2\pi y)$ as the preceding example. As demonstrated in Fig. 11, an asymptotic error toward a finite limit is observed. This is similar

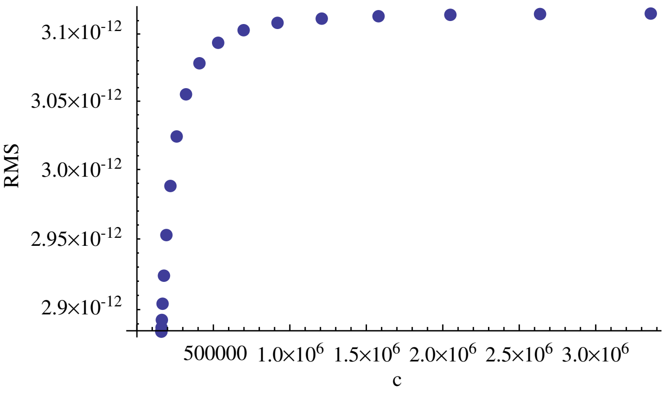

Fig. 7. RMS error $\varepsilon_{\mathrm{RMS}}(s,u)$ for solution of PDE with exact solution $u(x,y)=\sin(2\pi x)+\cos(2\pi y)$ using IMQ: mesh size $h=1/20$, in large c range.

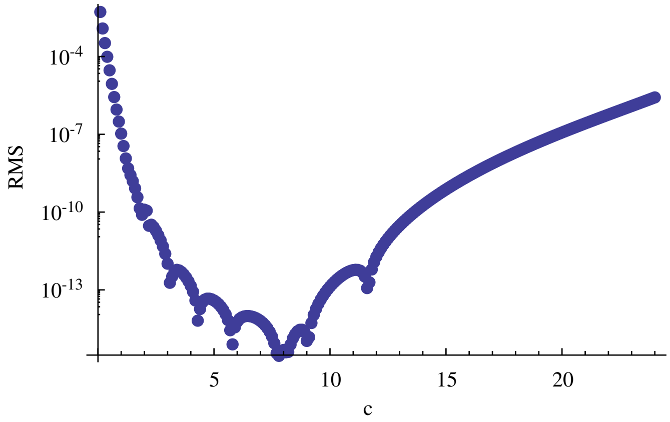

Fig. 9. RMS error $\varepsilon_{\mathrm{RMS}}(s,u)$ for solution of PDE with exact solution $u(x,y)=\sin(2\pi x)\cos(2\pi y)$ using IMQ: mesh size $h=1/20$, in smaller c range.

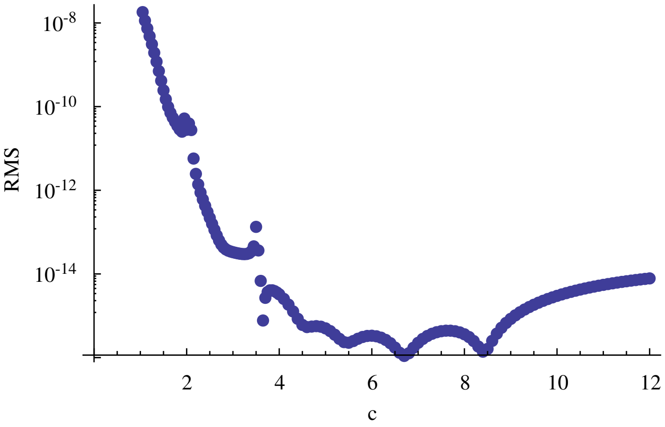

Fig. 8. RMS error $\varepsilon_{\mathrm{RMS}}(s,u)$ for solution of PDE with exact solution $u(x,y)=\sin(2\pi x)+\cos(2\pi y)$ using IMQ: mesh size $h=1/20$, in smaller c range.

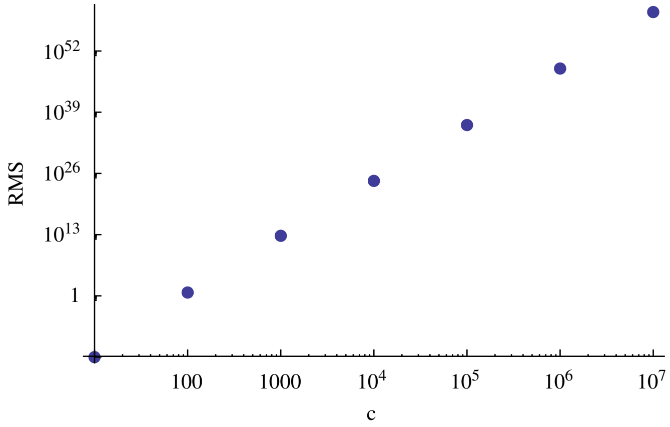

Fig. 10. RMS error $\varepsilon_{\mathrm{RMS}}(s,u)$ for solution of PDE with exact solution $u(x,y)=\sin(2\pi x)\cos(2\pi y)$ using IMQ: mesh size $h=1/20$, in large c range.

Please cite this article as: Huang C-S, et al. On the increasingly flat radial basis function and optimal shape parameter for the solution of elliptic PDEs. Eng Anal Bound Elem (2010), doi:10.1016/j.enganabound.2010.03.002

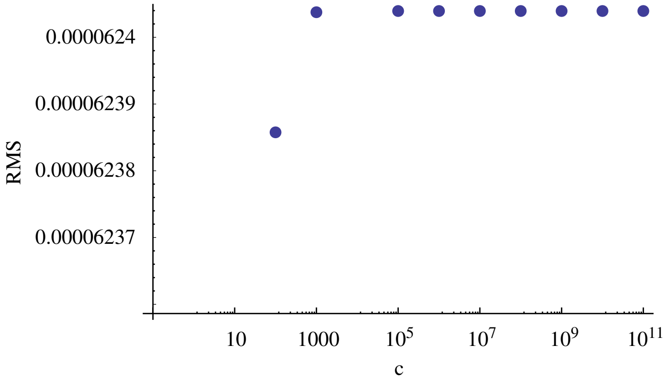

Fig. 11. RMS error $\varepsilon_{\mathrm{RMS}}(s,u)$ for solution of PDE with exact solution $u(x,y)=\sin(2\pi x)\cos(2\pi y)$ using GA: mesh size $h=1/10$, in large c range.

to the interpolation problem using GA, i.e., Example 5.1, but dissimilar to the solution of PDE using IMQ, Example 6.2, which diverges. As compared to Fig. 6 for the interpolation case, the asymptotic limit is a few fold larger for the PDE case.

We have also tested a few other bivariate transcendental functions, involving exponential functions, such as $\exp(10\sqrt{x^2+y^2})$, and the product of trigonometric functions, such as $u(x,y)=\sin(\pi x/6)\sin(7\pi x/4)\sin(3\pi y/4)\sin(5\pi y/4)$, using IMQ and GA as basis functions. We observe that as $\epsilon\to 0$, the IMQ interpolants diverge on uniform grid, while the GA interpolants converge. This suggests that the theorem of Fornberg et al. [17], which states that for interpolation, GA interpolants will always converge as $\epsilon\to 0$, whatever the grid arrangement, may be extended to the PDE solution case.

7. Random grid

Driscoll and Fornberg [16] suggested that for two-dimensional interpolation problems, irregular grid layout for collocation points always results in polynomial interpolation. This motivates us to test the same conjecture for PDE solution. However, rather than using a random selection of collocation nodes from a regular grid system, we randomly disturb the node locations from a regular grid layout. This is described as the following:

(1) Given a uniform layout of collocation point set $\Omega^o=\{(x_i,y_j)|1\le(i,j)\le N\}$, along the Cartesian coordinates, with spacing h, we choose a positive real number, $\delta\le h/2$, to perturb each $(x_i,\ y_j)$ within a disk $D(x_i,y_j,\delta)=\{(x,y)|\sqrt{(x-x_i)^2+(y-y_j)^2}<\delta\}$. Note that the adjacent disks will not intersect each other, since $\delta\le h/2$.

(2) We then create N random numbers, $0\le m_{ij}\le 1$, and N random angles $0\le\theta_{ij}\le 2\pi$, and set our new random collocation points to be $\Omega^o_\delta=\{(x_i^*,y_j^*)|x_i^*=x_i+m_{ij}\delta\cos(\theta_{ij}),y_j^*=y_j+m_{ij}\delta\sin(\theta_{ij})\}$.

7.1. Example 7.1

Using this random grid generation process, and a uniform grid size $h=1/10$, we select four different perturbation radius, $\delta=h/2$, $h/10$, $h/100$, $h/1000$. For each of the perturbation radius, we create five random collocation node data sets, and denote them by $\{\Omega^o_{\delta,i},\ i=1,\ldots,5\}$. Now we take $\Omega^o_{\delta,i}$ as our collocation points and solve the boundary value problem of Poisson's equation over $[0,1]\times[0,1]$, with the exact solution $u(x,y)=\sin(\pi x/6)\sin(7\pi x/4)\sin(3\pi y/4)\sin(5\pi y/4)$, using IMQ as the basis function. A summary of the results is reported in Tables 5–7. In these tables, we report only the limit of the RMS error as $c\to\infty$ (if it exists), the optimal c value, and the minimum error associated with it.

First, we observe from these tables that the RMS error converged to finite limits for all these random collocation node cases. Here we are reminded that for a uniform grid, it will diverge. From Table 5, we observe that a convergence can be achieved with a very small perturbation of nodes, with perturbation radius of only $\delta=h/1000$.

From Tables 5–7, we observe that, if we locate the optimal c value, the minimum error can be 2 to 4 orders of magnitude smaller than the polynomial limit. We also find from Tables 6 and 7 that, as the perturbation radius grows to a significant size, the minimum error decreases. This fact is further illustrated in

Table 5
RMS error in the limit of $c\to\infty$, optimal c, and minimum error for five different collocation sets with $\delta=h/1000$.

Collocation set	$\varepsilon_{\mathrm{RMS}}$ as $c\to\infty$	optimal c	optimal $\varepsilon_{\mathrm{RMS}}$
$\Omega^o_{h/1000,1}$	2.526(−2)	2.70	5.221(−6)
$\Omega^o_{h/1000,2}$	2.721(−2)	2.50	3.050(−6)
$\Omega^o_{h/1000,3}$	7.296(−3)	3.44	3.804(−6)
$\Omega^o_{h/1000,4}$	6.608(−2)	2.56	4.054(−6)
$\Omega^o_{h/1000,5}$	9.793(−3)	2.56	4.543(−6)

Table 6
RMS error in the limit of $c\to\infty$, optimal c, and minimum error for five different collocation sets with $\delta=h/10$.

Collocation set	$\varepsilon_{\mathrm{RMS}}$ as $c\to\infty$	Optimal c	optimal $\varepsilon_{\mathrm{RMS}}$
$\Omega^o_{h/10,1}$	2.528(−2)	4.00	1.104(−6)
$\Omega^o_{h/10,2}$	2.527(−4)	2.38	2.452(−6)
$\Omega^o_{h/10,3}$	6.772(−4)	2.87	1.105(−6)
$\Omega^o_{h/10,4}$	5.271(−3)	2.43	7.473(−7)
$\Omega^o_{h/10,5}$	2.867(−4)	2.77	7.149(−7)

Table 7
RMS error in the limit of $c\to\infty$, optimal c, and minimum error for five different collocation sets with $\delta=h/2$.

Collocation set	$\varepsilon_{\mathrm{RMS}}$ as $c\to\infty$	Optimal c	Optimal $\varepsilon_{\mathrm{RMS}}$
$\Omega^o_{h/2,1}$	1.903(−4)	2.70	4.374(−7)
$\Omega^o_{h/2,2}$	2.134(−4)	4.00	3.466(−7)
$\Omega^o_{h/2,3}$	3.820(−5)	4.00	5.158(−7)
$\Omega^o_{h/2,4}$	6.187(−5)	3.84	5.392(−7)
$\Omega^o_{h/2,5}$	1.349(−3)	4.00	4.814(−7)

Table 8
RMS errors and optimal c and optimal RMS errors of RBF interpolation with $r=h/2$, $h/10$, $h/100$, $h/1000$.

Collocation set	$\varepsilon_{\mathrm{RMS}}$ as $c\to\infty$	optimal c	optimal $\varepsilon_{\mathrm{RMS}}$
$\Omega^o_{h/1000,1}$	7.868(−3)	2.6	3.781(−7)
$\Omega^o_{h/100,1}$	7.702(−4)	2.8	4.771(−7)
$\Omega^o_{h/10,1}$	1.904(−4)	2.9	2.504(−7)
$\Omega^o_{h/2,1}$	3.833(−5)	2.7	1.026(−7)

Table 8, where we compile cases of different perturbation radius, with Ω_0^o representing the uniform grid case ($\delta = 0$). We observe that the optimal c value largely remains a constant, while both the polynomial error limit and the optimal error generally decrease when the perturbation radius is increased.

8. Conclusions

Based on the above numerical study, we may draw the following conclusions/conjectures:

- For one-dimensional interpolation problems, as well as for the solution of boundary value problems of ordinary differential equations, using a class of infinitely smooth basis functions that can be expanded into a power series (12), the interpolant (4) converges to a polynomial limit as the basis functions are continuously flattened by taking $\in \to 0$. The asymptotic error is of the order $\mathcal{O}(\in^2)$. This class of basis functions includes the IMQ, GA, MQ and IQ, as presented in Tables 1 and 2, as well as other basis functions. For the interpolation case, the above conclusion is in fact the theoretical result of Driscoll and Fornberg [16].
- When such a finite error limit exists, the minimum error is generally not found at this limit; rather, the minimum error can be located at some finite c value. This statement is true for one- and multi-dimensional problems, and for interpolation as well as for solution of PDE.
- The error pattern, which includes the convergent/divergent behavior as $c \to \infty$ and the existence of an optimal c associated with minimum error, is generally the same for the interpolation and for the solution of PDE problems, for the same type of function approximated, and the same basis function used.
- The error associated with the solution of PDE is generally larger than that associated with interpolation of function.
- For IMQ, the interpolant can diverge or converge on uniform grid or certain regular node pattern, as $\in \to 0$. Whether the interpolant diverges or not is dependent on the function interpolated. Based on the observation in this paper, the interpolant converges for essentially one-dimensional functions and multivariate polynomials. In the latter case, the error converges to zero. Divergent behavior is observed for all other functions tested.
- The IMQ interpolant becomes convergent as $\in \to 0$ for all functions, when the nodes are randomly perturbed from a uniform grid.
- For the interpolation and the solution of PDE problems, GA interpolant converges for all functions and all interpolation node arrangement, as $\in \to 0$. The case for interpolation is a conjecture of Fornberg et al. [17].
- The GA interpolant can typically achieve somewhat better accuracy than the IMQ.

References

[1] Franke R. Scattered data interpolation—tests of some methods. Math Comput 1982;38:181–200.

[2] Hardy RL. Multiquadric equations of topography and other irregular surfaces. J Geophys Res 1971;76:1905–15.

[3] Hardy RL. Theory and applications of the multiquadric-biharmonic method—20 years of discovery. Comput Math Appl 1990;19:163–208.

[4] Kansa EJ. Multiquadrics—a scattered data approximation scheme with applications to computational fluid-dynamics. 1. Surface approximations and partial derivative estimates. Comput Math Appl 1990;19:127–45.

[5] Kansa EJ. Multiquadrics—a scattered data approximation scheme with applications to computational fluid-dynamics. 2. Solutions to parabolic, hyperbolic and elliptic partial-differential equations. Comput Math Appl 1990;19:147–61.

[6] Hon YC, Cheung KF, Mao XZ, Kansa EJ. Multiquadric solution for shallow water equations. J Hydraul Eng ASCE 1999;125:524–33.

[7] Hon YC, Lu MW, Xue WM, Zhu YM. Multiquadric method for the numerical solution of a biphasic mixture model. Appl Math Comput 1997;88:153–75.

[8] Vertnik R, Sarler B. Meshless local radial basis function collocation method for convective–diffusive solid–liquid phase change problems. Int J Numer Methods Heat & Fluid Flow 2006;16:617–40.

[9] Wen PH, Hon YC. Geometrically nonlinear analysis of Reissner–Mindlin plate by meshless computation. Comput Modeling Eng & Sci 2007;21:177–91.

[10] Cheng AH-D, Cabral JJSP. Direct solution of ill-posed boundary value problems by radial basis function collocation method. Int J Numer Methods Eng 2005;64:45–64.

[11] Tarwater AE. Parameter study of Hardy's multiquadric method for scattered data interpolation. Technical Report UCRL-54670; 1985, 69p.

[12] Madych WR. Miscellaneous error-bounds for multiquadric and related interpolators. Comput Math Appl 1992;24:121–38.

[13] Cheng AH-D, Golberg MA, Kansa EJ, Zammito G. Exponential convergence and h–c multiquadric collocation method for partial differential equations. Numer Methods Partial Diff Eqns 2003;19:571–94.

[14] Huang C-S, Lee C-F, Cheng AH-D. Error estimate, optimal shape factor, and high precision computation of multiquadric collocation method. Eng Anal Boundary Elem 2007;31:614–23.

[15] Baxter BJC. The asymptotic cardinal function of the multiquadratic $f(r) = (r^2 + c^2)^{1/2}$ as $c \to \infty$. Comput Math Appl 1992;24:1–6.

[16] Driscoll TA, Fornberg B. Interpolation in the limit of increasingly flat radial basis functions. Comput Math Appl 2002;43:413–22.

[17] Fornberg B, Wright G, Larsson E. Some observations regarding interpolants in the limit of flat radial basis functions. Comput Math Appl 2004;47:37–55.

[18] Larsson E, Fornberg B. Theoretical and computational aspects of multivariate interpolation with increasingly flat radial basis functions. Comput Math Appl 2005;49:103–30.

[19] Schaback R. Multivariate interpolation by polynomials and radial basis functions. Constructive Approximation 2005;21:293–317.

[20] Fairweather G, Karageorghis A. The method of fundamental solutions for elliptic boundary value problems. Adv Comput Math 1998;9:69–95.

[21] Bogomolny A. Fundamental-solutions method for elliptic boundary-value problems. SIAM J Numer Anal 1985;22:644–69.

[22] Chen JT, Lee YT, Yu SR, Shieh SC. Equivalence between the Trefftz method and the method of fundamental solution for the annular Green's function using the addition theorem and image concept. Eng Anal Boundary Elem 2009;33:678–88.

[23] Schaback R. Adaptive numerical solution of MFS systems. In: Chen CS, Karageorghis A, Smyrlis YS, editors. The method of fundamental solutions—a meshless method. Atlanta, GA, Dynamic Publishers; 2008. p. 1–27. [chapter 1].

[24] Li Z-C, Lu Z-Z, Hu H-Y, Cheng AH-D. Trefftz and collocation methods. Southampton, Boston, WIT Press; 2008.

[25] Kolodziej JA, Zielinski AP. Boundary collocation techniques and their application in engineering. Southampton, Boston, WIT Press; 2009.

[26] Buhmann MD. Radial basis functions: theory and implementations. Cambridge, UK, Cambridge University Press; 2003.

[27] Wendland H. Scattered data approximation. Cambridge, UK, Cambridge University Press; 2005.

[28] Micchelli CA. Interpolation of scattered data—distance matrices and conditionally positive definite functions. Constructive Approximation 1986;2:11–22.

[29] Yen H-D. On the increasingly flat RBFs based solution methods for elliptic PDEs and interpolations. Master thesis, Department of Applied Mathematics, National Sun Yat-Sen University, Taiwan; 2008, 70p.

Please cite this article as: Huang C-S, et al. On the increasingly flat radial basis function and optimal shape parameter for the solution of elliptic PDEs. Eng Anal Bound Elem (2010), doi:10.1016/j.enganabound.2010.03.002